Pharmacogn. Mag.
A multifaceted peer reviewed journal in the field of Pharmacognosy and Natural Products
www.phcog.com | www.phcog.net

ORIGINAL ARTICLE

Aloperine Improves Renal Fibrosis via Regulation of Toll-Like Receptor 4/Myeloid Differentiation Factor 88 Signaling Pathway

Zhen-Tian Cheng, Xiang-Ping Yuan[1]

Department of Medicine, Yidu Central Hospital of Weifang, [1]Department of Kidney Medicine, Yidu Central Hospital of Weifang, Qingzhou, China

Submitted: 19-May-2020 Revised: 15-Jul-2020 Accepted: 16-Feb-2021 Published: 11-Nov-2021

ABSTRACT

Objectives: The primary goal of this study was to elucidate the effects and mechanisms of aloperine (Alo) in the renal fibrosis mice with unilateral ureteral obstruction (UUO). **Materials and Methods:** C57BL/6 mice were randomly separated into five groups: sham, model, Alo-L, Alo-M, and Alo-H. Serum creatinine and blood urea nitrogen were measured by chemical methods. The histopathological changes and collagen deposition in the affected kidney were evaluated under optical microscope by performing hematoxylin and eosin and Masson staining. The expression of alpha smooth muscle actin, fibronectin, Toll-like receptor (TLR)-4, and myeloid differentiation factor 88 (MyD88) proteins was evaluated by immunohistochemistry, and the protein expression of interleukin (IL)-6 and tumor necrosis factor (TNF)-α was evaluated via Western blot analysis. **Results:** The degree of fibrosis and histopathological damage was most clear in the kidney tissues obtained from model group. Furthermore, the expression of TLR4 and MyD88 was the maximum in the model group. However, Alo decreased the injury to the kidney, thereby improving their condition. It also decreased the levels of terminal inflammatory cytokines (i.e., TNF-α and IL-6). **Conclusion:** Alo may progress renal fibrosis by inhibiting TLR4/MyD88 pathway.

Key words: Aloperine, immune and inflammatory responses, renal fibrosis, Toll-like receptor 4/myeloid differentiation factor 88 pathway, unilateral ureteral ligation

SUMMARY

- Toll-like receptor (TLR4)/myeloid differentiation factor 88 (MyD88) activation plays an important role in renal fibrosis
- Aloperine improves renal fibrosis via TLR4/MyD88 signaling pathway.

Abbreviations used: Alo: Aloperine; UUO: Unilateral ureteral obstruction; IHC: Immunohistochemistry; WB: Western Blotting; ELISA: Enzyme-linked immunosorbent assay; TNF-α: Tumor necrosis factor-α; IL-6: Interleukin-6; H and E staining: Hematoxylin and eosin staining; TLR4: Toll-like receptor 4; MyD88: Myeloid differentiation factor 88.

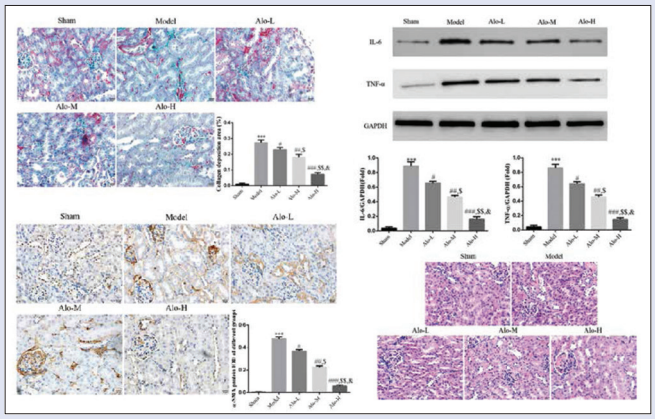

Correspondence:

Dr. Zhen-Tian Cheng,
Department of Medicine, Yidu Central Hospital of Weifang, 4138 Linglongshan South Road, 262500 Qingzhou, China.
E-mail: lanxinqiang0731@163.com

DOI: 10.4103/pm.pm_137_20

Access this article online
Website: www.phcog.com
Quick Response Code:

INTRODUCTION

The pathogenesis of renal fibrosis is progressive in the case of nearly all kidney diseases, which culminates into the end-stage renal failure. It is more likely to cause progressive worsening of renal function as compared to primary renal diseases. It is a direct significance of the kidney's limited capacity to regenerate after injury.[1] Renal fibrosis is driven by multiple factors, involving inflammation, oxidative stress, various cytokines, apoptosis, fibroblast proliferation and activation, and transformation of epithelial cells into fibroblasts.[2] Treatment of renal fibrosis is of utmost priority to the medical fraternity. So far, Traditional Chinese Medicine (TCM) has proved to be effective in the treatment of renal fibrosis.[3-6]

Aloperine (Alo) is an alkaloid extracted from *Sophora alopecuroides* L. In TCM, it is used as an anti-inflammatory, anticancer, and antibacterial agent.[7] Many studies have reported that Alo can reduce neuropathic pain caused by chronic compressive injury and protect against hippocampal neuronal damage caused by oxygen deprivation and reperfusion.[8,9] A recent study has established that Alo can reduce acute kidney injury caused by ischemia–reperfusion.[10] A preliminary study has established that the inflammatory response mediated by Toll-like receptor (TLR)-4 is involved in the process of renal interstitial fibrosis, and its expression increases along with the severity of renal interstitial fibrosis.[11] Other studies have also shown that activation of macrophages, dendritic cells, and undifferentiated fibroblasts in mice with a deficiency of TLRs can impede fibroblast infiltration, thereby reducing the degree of renal fibrosis.[12] In this study, unilateral ureteral obstruction (UUO) model was employed to persuade renal interstitial fibrosis, and the effects of Alo in treating renal interstitial fibrosis and its mechanism related to TLR signaling pathways were further explored.

Cite this article as: Cheng ZT, Yuan XP. Aloperine improves renal fibrosis via regulation of Toll-like receptor 4/myeloid differentiation factor 88 signaling pathway. Phcog Mag 2021;17:587-93.

MATERIALS AND METHODS

Experimental animals

A total of 50 healthy adult C57BL/6 mice weighing around 20 ± 5 g were acquired from Chengdu Dossy Experimental Animals Co. Ltd. (License number: SCXK [Sichuan] 2015-030). The mice were housed in the Renal Function Protection Experimental Center of Southwest Medical University and were provided with free drinking water and standard routine food. They were exposed to 12-h light and 45% humidity.

Main drugs and reagents

Aloperine (Alo) was purchased from Ningxia Bauhinia Pharmaceutical Co., Ltd., with a purity of 99%; 1% pentobarbital sodium (Beijing Chemical Reagent, China); SPV immunohistochemistry detection kit (Beijing Zhongshang Jinqiao Biotechnology Co., Ltd., China); ECL detection kit (Jiangsu Kaiji Biotechnology Co., Ltd., Nanjing, CHina); HE and Masson staining kits were purchased from Solvay Biotech Co., Ltd.(Beijing, China); DAB color development kit, creatinine (Cr) detection kit, and blood urea nitrogen (BUN) detection kit were purchased from Maixin Technology Co., Ltd. (Hanzhou, China); Western blotting equipment (BioRAD, Herocules, CA, USA); TLR4 antibody (Abcam, Cambridge, MA, USA); Myeloid differentiation factor 88 (MyD88) antibody (Cell Signaling Technology); alpha smooth muscle actin (α-SMA) antibody (Sigma, Rockville, MD, USA); Fibronectin antibody and interleukin-6 (IL-6) antibody (Boster Biological Technology, Wuhan); Tumor necrosis factor-α (TNF-α) antibody (Abcam, Rockville, MD, USA); GAPDH (Beyotime Biotechnology, Shanghai, China).

Instruments

Polymerase chain reaction amplification instrument (Gene); gel electrophoresis apparatus and gel imager (Bio-Rad); absorbing light microplate reader (Biotek); inverted phase contrast microscope (Olympus); micronucleic acid meter (Gene); low-temperature high-speed centrifuge (Eppendorf); and paraffin slicer (Leica) were used during the study.

Unilateral ureteral obstruction model preparation

The animals were anesthetized via intraperitoneal injection with 1% pentobarbital sodium. Then, the mice were shaved, sterilized, and covered with a towel. The animals were fixed on the operation table in the right lateral position. A longitudinal cut was made on the left abdomen, and the skin was cut to the abdominal cavity to depict the kidney. Both sides of the slit were covered with a saline-soaked gauze. Once the ureter was recognized, the left ureter was separated, leaving it in a free state. The renal pelvis and one-third of the ureter were ligated with silk thread, and then, the ureter was cutoff at the ligature. After the operation, the kidney and ureter were repaid to their original positions, and the layers of muscle and skin were successively sutured. Same steps were performed for the sham group, except for ligating the ureter.

Grouping and dosing

The mice were randomly divided into five groups: The model group, the Alo high-dose, medium-dose, low-dose (40, 20, and 10 mg/kg) group, and the sham group. The UUO model was recognized in the model group and the Alo groups. The same steps were performed for the sham group, except for ligating the ureter. After surgery, the Alo groups were given IG Alo solution, whereas the model and sham groups were given the same volume of normal saline once a day for 14 days. All mice were fed and caged as clean animals. The mice were given free admittance to water and food at a temperature of 23°C ± 2°C and a relative humidity of 55% ± 2%.

Sampling

On post-operation day 14, the blood was composed from the heart, allowed to stand for 30 min, and centrifuged at 3000 rpm for 10 min. The supernatant was collected for testing. Left kidney tissue was collected and partly stored in 4% paraformaldehyde solution. After the sample was embedded in paraffin, it was subjected to H and E and Masson staining and IHC. The remaining kidney tissue was quickly cooled with liquid nitrogen and stored in a refrigerator at −80°C for the extraction of protein.

Determination of blood creatinine and blood urea nitrogen levels

Serum was occupied and the absorbance (A) value of the corresponding band was measured by a microplate reader using a detection kit to measure the serum Cr and BUN levels.

Renal tissue hematoxylin and eosin and Masson staining

The paraffin-embedded renal tissue was exposed to H and E and Masson staining, according to the conventional method. The Masson-stained tissue slices[13] were taken and 10 different fields of view (×400-fold) were designated for each slice. Blue collagen deposition was taken as a positive signal. Image Pro Plus image processing software was employed for analysis. The ratio of the renal interstitial collagen deposition area to the total area of renal tubulointerstitial in the field of view was considered and the average was achieved.

Immunohistochemistry staining for detection of related protein expressions

The expressions of TLR4, MyD88, α-SMA, and fibronectin in the mouse renal tissue were distinguished by SPV. The renal tissues of each group were taken and entrenched in paraffin. The samples were sliced in 5 μm thick each, baked for 2 h, and regularly dewaxed and rehydrated. They were treated with 1% hydrogen peroxide solution at 37°C for 10 min. After heat-repairing with antigen-repairing solution, the samples were obviously cooled to room temperature and incubated with antibody overnight at 4°C. The primary antibody was replaced by 5% rabbit serum as a blank control. After 12 h, reagent 1 was added (following kit instructions). After incubation at 37°C for 20 min, reagent 2 was added (following kit instructions) and the samples were incubated again at 37°C for 20 min. After DAB color development for 8 min, hematoxylin staining for 5 min, and dehydration by gradient alcohol for 1 min each, the samples were deparaffinized with xylene and sealed with neutral gum. The yellowish-to-brown tissues were absolutely stained. Image Pro Plus was used for image analysis. In the 10 non-overlapping 400-fold fields of view of each slice, the ratio of the positively stained area to the total tubulointerstitial area in the field of view was calculated and the average was obtained.

Western blot analysis for the detection of related protein expressions

According to the molecular experimental guidelines, the total protein was removed and the protein concentration was quantified by bicinchoninic acid method. The proteins were detached by electrophoresis in 10% sodium dodecyl sulfate-polyacrylamide gel (SDS-PAGE) and wet

transferred onto polyvinylidene fluoride (PVDF) membrane. Then, the samples were wrapped with 5% skim milk at room temperature for 1 h, added with primary antibody, shaken at room temperature for 30 min, and stored overnight at 4°C. PBST was used to wash the membrane for three times, 10 min each time. Then, the samples were added with equivalent secondary antibody, shaken at room temperature for 1 h, and eroded with PBST. ECL test solution was used for autoradiography. The development results were analyzed by the integral absorbance value using Quantity One software, and the results were corrected by GAPDH. The antibodies were diluted to the following ratios: IL-6 (1:1000), TNF-α (1:1000), and GAPDH (1:1000).

Statistical methods

SPSS 17.0 software was used for statistical analysis. All results were articulated as mean ± standard deviation. The *t*-test was used for comparison between two groups, while the one-way analysis of variance and Student–Newman–Keuls-*q* test were used for comparison between multiple groups. All experiments were repetitive at least three times. A $P < 0.05$ was measured statistically significant.

RESULTS

Renal functional changes

There was no substantial difference in the serum Cr and BUN levels in all groups ($P > 0.05$) [Figure 1].

Renal histopathological changes

H and E staining [Figure 2] displays that, in the sham group, the structures of renal cortex and medulla were usual, the size and shape of the renal tubules and glomeruli were standard, and renal tubulointerstitial displays no broadening, obvious hyperemia, and inflammatory cell infiltration. On the 14th day after the operation, mice in the model group were found with significantly augmented volume of the left kidney, prolonged renal pelvis and calyx, and thinned renal parenchyma. Under the optical microscope, variable degrees of tubular dilatation and denatured shedding of the epithelial cell were detected. The renal interstitial could be witnessed with varying degrees of edema and inflammatory cell infiltration. Some glomeruli had varying degrees of atrophy or even vanished. There were obvious manifestations of renal interstitial fibrosis, such as widened renal interstitial and increased collagen deposition. However, in the Alo group, the renal interstitial edema, glomerular atrophy, and inflammatory cell infiltration were not as noteworthy as those in the model group, with a certain degree of renal interstitial broadening.

Masson staining changes

Masson staining [Figure 3] illustrated that in the sham group, collagen staining mainly happened at the tubular basement membrane and around the tubule, while renal tubulointerstitial staining was hardly detected. Compared with the sham group, the model group was found with dilated tubular, broadened renal interstitial, and suggestively increased collagen content. The degree of the renal interstitial collagen deposition was abridged in the Alo groups, compared with the model group ($P < 0.001$, respectively), as shown in Figure 3. This shows that UUO caused fibrosis in the affected kidney after 14 days, while Alo could significantly reduce and improve the degree of renal fibrosis in mice after UUO. Meanwhile, the deposition of the renal interstitial collagen could be dose-dependently abridged.

Renal tissue alpha smooth muscle actin and fibronectin changes

The results of IHC and image analysis of α-SMA and fibronectin [Figures 4 and 5] show that both α-SMA and fibronectin-positive staining areas were largely intercellular. The expression of α-SMA and fibronectin was higher in the model group than that in the sham and Alo groups ($P < 0.001$), signifying that the degree of renal fibrosis in the model group was greater than that in the sham and Alo groups. The degree of renal fibrosis in the Alo group was reduced compared with the model group ($P < 0.001$, respectively), and the reduction was dose dependent.

Immunohistochemistry for Toll-like receptor 4 and myeloid differentiation factor 88 protein expression

According to the results of IHC along with semiquantitative analyses [Figures 6 and 7], TLR4-positive staining area was mainly situated in the cell membrane, and the MyD88-positive staining was mainly located in the cytoplasm. Their expressions were higher in the model group than that in the sham and Alo groups ($P < 0.001$, respectively). The expression of these proteins was lower in the Alo group than that in the model group ($P < 0.001$, respectively), and there was a dose-dependent relationship. There were significantly differences between sham and Model groups in TLR4 expression, this results had showed that the increased expression of TLR4 was positively correlated with fibrosis, confirming that the immune inflammatory responses mediated by TLR4 are involved in the process of renal interstitial fibrosis. Moreover, TLR4/MyD88 pathway activating was correlation with renal fibrosis increasing. As the concentration of Alo increased, the expression

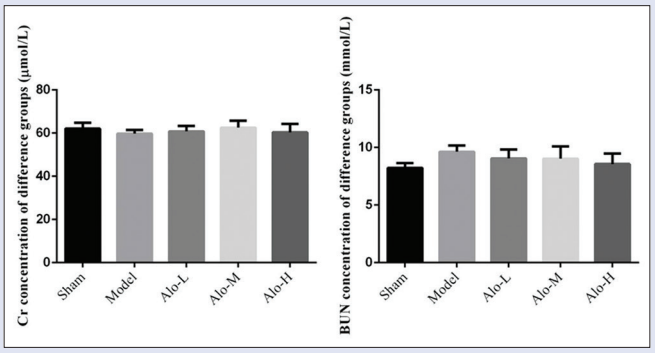

Figure 1: Effect of aloperine on creatinine and blood urea nitrogen in serum of unilateral ureteral obstruction mice (mean ± standard deviation, $n = 10$)

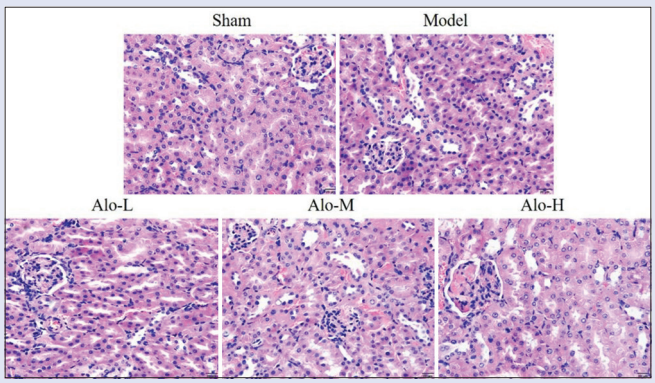

Figure 2: Results of mouse kidney (H and E, ×400)

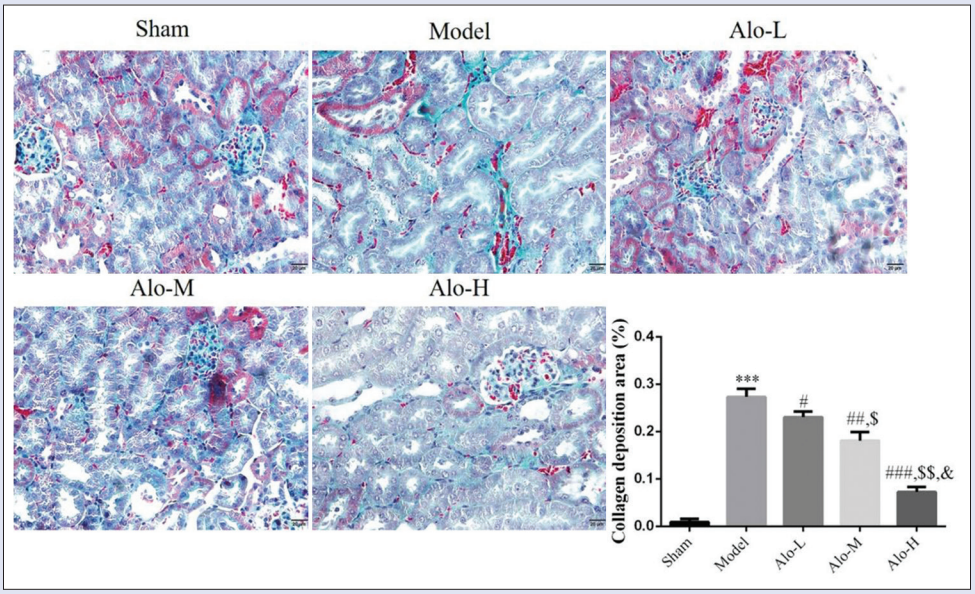

Figure 3: Masson staining of mouse kidney (×400). ***: $P < 0.001$, compared with sham group; #: $P < 0.05$; ##: $P < 0.01$; ###: $P < 0.001$, compared with model group; $: $P < 0.05$, $$: $P < 0.01$, compared with Alo-L group; and: $P < 0.05$, compared with Alo-M group

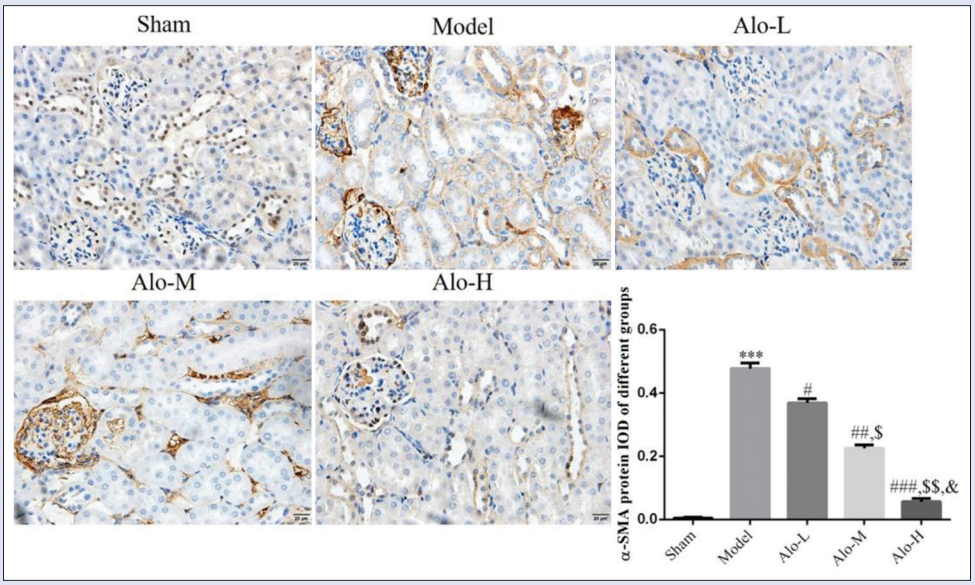

Figure 4: The alpha smooth muscle actin protein expression of difference groups by immunohistochemistry assay (×400). ***: $P < 0.001$, compared with Sham group; #: $P < 0.05$; ##: $P < 0.01$; ###: $P < 0.001$, compared with Model group; $: $P < 0.05$, $$: $P < 0.01$, compared with Alo-L group; and: $P < 0.05$, compared with Alo-M group

of proteins related to the TLR/MyD88-dependent signaling pathway slowly decreased, showing that Alo might alleviate renal fibrosis by regulating the TLR/MyD88-dependent signaling pathway.

Western blot analysis for changes in interleukin-6 and tumor necrosis factor-α proteins

According to our results [Figure 8], Alo group showed infiltration of inflammatory cytokines in the renal tissue, which was less severe than that in the model group ($P < 0.001$). Furthermore, the expression of IL-6 and TNF-α proteins [Figure 8] showed that Alo could alter the TLR/MyD88-dependent signaling pathway, thereby inhibiting the release of inflammatory cytokines at the end of this pathway. This shows that Alo shows anti-inflammatory activity.

DISCUSSION

The pathological variations of renal fibrosis can be seen during the chronic progression of the kidney disease. Reducing or even reversing renal fibrosis has been the eventual goal for the treatment of chronic kidney diseases. Alo is a quinolizidine alkaloid extracted from *S. alopecuroides* L. Studies have established that Alo can reduce the degree of renal fibrosis,[14] and it plays an important role in the treatment of many kidney diseases.[15,16]

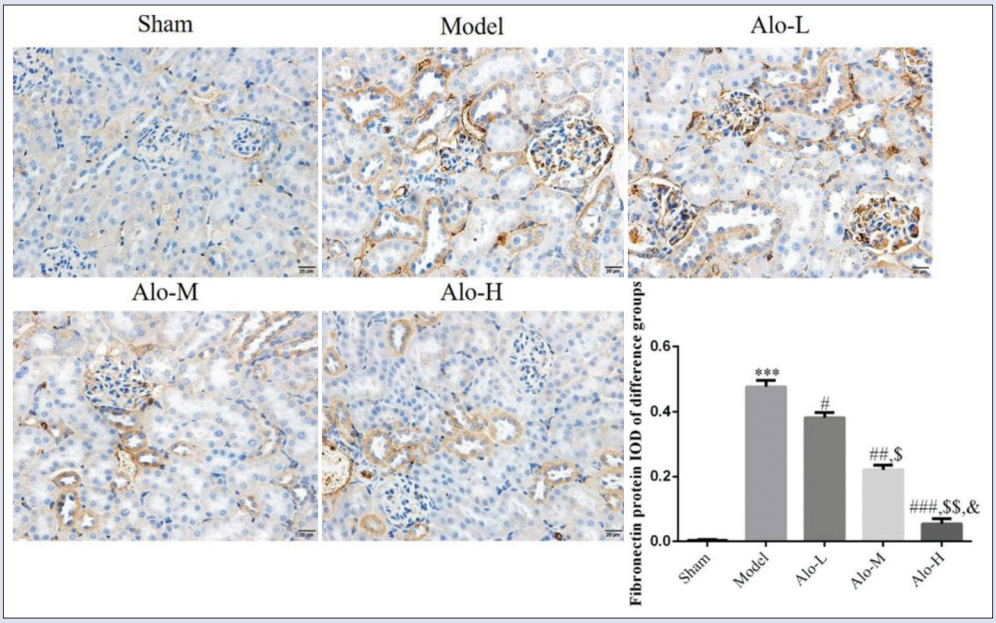

Figure 5: The fibronectin protein expression of difference groups by immunohistochemistry assay (×400). ***: $P < 0.001$, compared with Sham group; #: $P < 0.05$; ##: $P < 0.01$; ###: $P < 0.001$, compared with model group; $: $P < 0.05$, $$: $P < 0.01$, compared with Alo-L group; and: $P < 0.05$, compared with Alo-M group

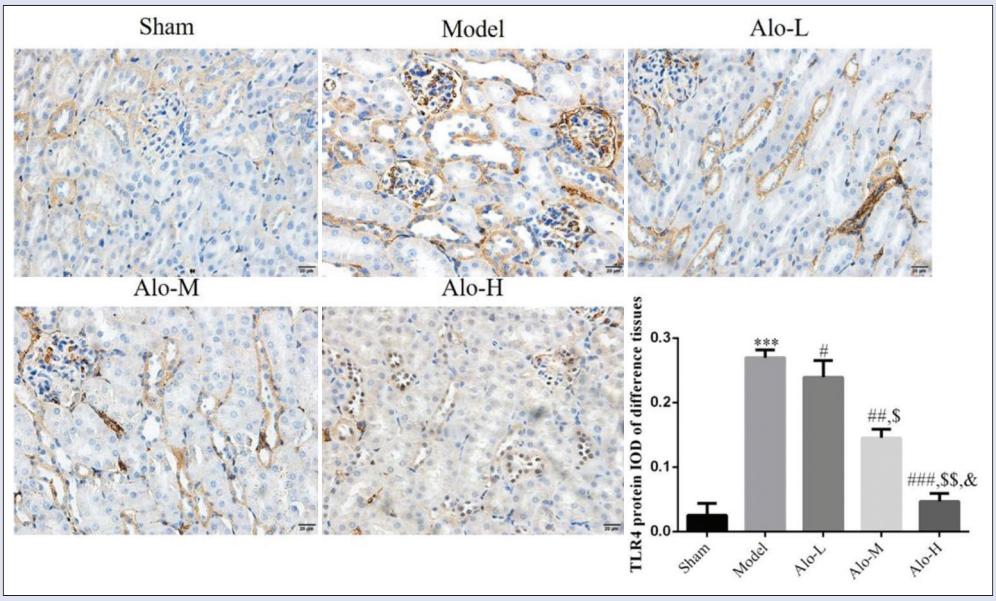

Figure 6: The Toll-like receptor 4 protein expression of difference groups by immunohistochemistry assay (×400). ***: $P < 0.001$, compared with Sham group; #: $P < 0.05$; ##: $P < 0.01$; ###: $P < 0.001$, compared with Model group; $: $P < 0.05$, $$: $P < 0.01$, compared with Alo-L group; and: $P < 0.05$, compared with Alo-M group

Renal fibrosis is a pathological condition of the kidneys, resulting from inflammation and injury. The mechanisms including ceelinflammatory changes, augmented extracellular matrix, and fibroblast accumulation.[17] However, TLRs have been as the primary factor of induced inflammation. They can activate pathogen- and damage-related patterns and stimulate the related signaling kinases via mediation of the intermediate adaptor protein, leading to the activation of transcription factors. TLRs activation can make inflammatory effector molecules transcribed and expressed, complete innate immune response or activate acquired immune response and inflammatory response, thus participating in acute and chronic renal tissue inflammation.[18] In signal cascade amplification, there are two types of pathways: MyD88-non-dependent and MyD88-non-dependent pathways. MyD88-dependent signal transduction pathway is a common pathway for all TLRs, except for TLR3, and it controls the secretion of IL-6, TNF, IFN-γ, IL-12, and IL-4.[19,20] In MyD88-dependent pathway, TLRs recruit and activate downstream-related signal kinases and TRAF-6 via MyD88, thereby activating mitogen-activated protein kinases and interferon regulatory factor 5 and completing the release of end inflammatory cytokines IL-1β and TNF-α with NF-κB pathway.[21] In the meantime, more research in

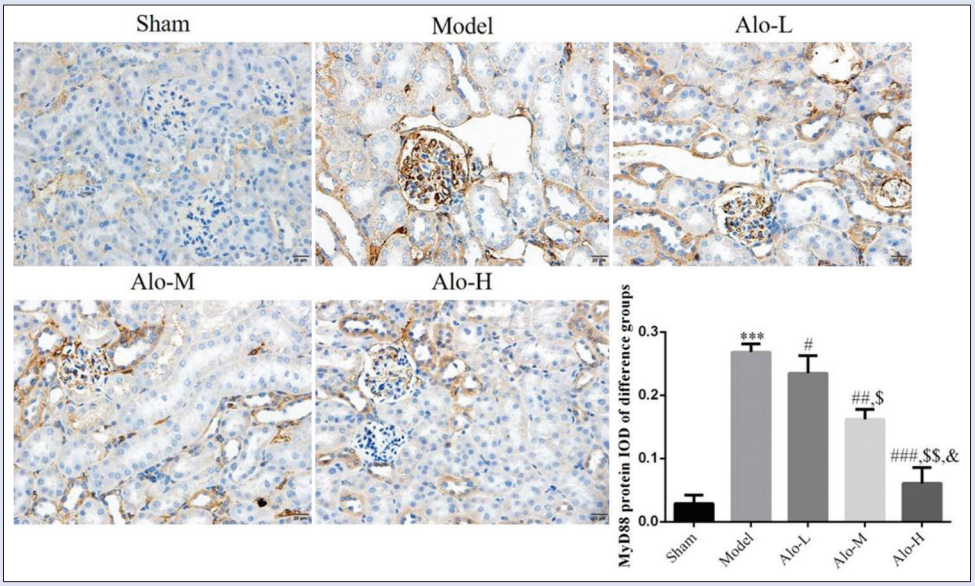

Figure 7: The myeloid differentiation factor 88 protein expression of difference groups by immunohistochemistry assay (×400). ***: $P < 0.001$, compared with Sham group; #: $P < 0.05$; ##: $P < 0.01$; ###: $P < 0.001$, compared with model group; $: $P < 0.05$, $$: $P < 0.01$, compared with Alo-L group; and: $P < 0.05$, compared with Alo-M group

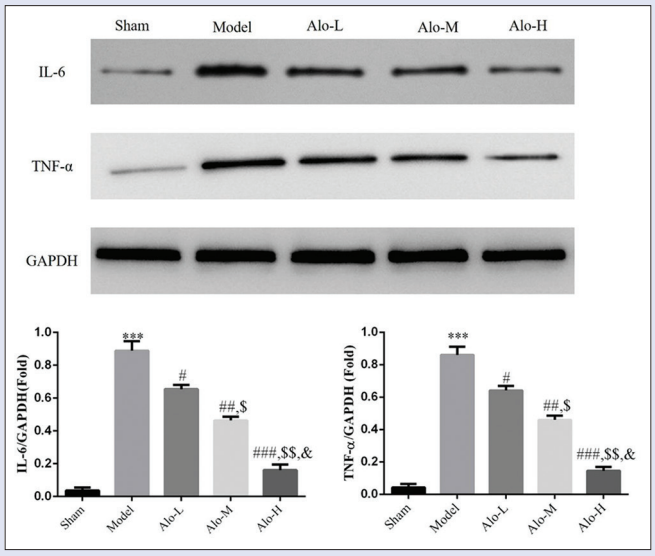

Figure 8: The interleukin-6 and tumor necrosis factor-α proteins expression by western blotting assay. ***: $P < 0.001$, compared with sham group; #: $P < 0.05$; ##: $P < 0.01$; ###: $P < 0.001$, compared with model group; $: $P < 0.05$, $$: $P < 0.01$, compared with Alo-L group; and: $P < 0.05$, compared with Alo-M group

this field has revealed that TLR4, TLR2, and TLR7 receptors and MyD88 have a profibrotic effect in the kidneys, and high expression of TLR9 can lessen the renal fibrosis.[22-28] In this study, TLR4 and MyD88 were employed to perceive the important nodes of this pathway so that we can reproduce the changes of the TLR/MyD88-dependent signaling pathway in the inflammatory response where UUO caused renal fibrosis in mice. In addition, the end inflammatory cytokines (IL-6 and TNF-α) were found to reproduce the regulation of the signaling pathway on the inflammatory cytokines.

The results of this study show that the levels of serum Cr and BUN were similar in all groups ($P > 0.05$), and the variance was not statistically significant. The possible reason is that the healthy kidney on the other side might reimburse for the injury on the exaggerated side, and there was no clear clinical appearance of the renal function.

In this study, Masson staining revealed that UUO instigated meaningfully augmented collagen content in the exaggerated kidney in the model group, and the degree of deposition of collagen in the renal interstitial tissue was lower in the Alo and sham groups than that in the model group ($P < 0.001$). According to the semi-quantitative results of IHC of α-SMA and fibronectin, the protein expression was downregulated in the Alo and the sham groups when compared with the model group ($P < 0.001$). According to the quantitative analysis of IHC of α-SMA, the protein expression was upregulated in the model group when compared with the sham group ($P < 0.05$). This shows that Alo could significantly reduce the degree of the renal fibrosis caused by UUO, and the effect was found to concentration dependent.

Results of IHC of the upstream molecules of the TLR/MyD88-dependent signaling pathway revealed that the expression of protein was considerably higher in the model group than that in the sham and Alo groups ($P < 0.001$). In particular, the protein expressions of TLR4 and MyD88 were similar in the medium-dose and high-dose groups, as well as in the sham group ($P > 0.001$). This shows that the protein expression related to the TLR/MyD88-dependent signaling pathway is correlated with the degree of the renal fibrosis on the exaggerated side of the mice. The expressions of TLR4 and MyD88 might increase the renal fibrosis, whereas Alo could constrain the expression of important node molecules in the TLR/MyD88-dependent signaling pathway.It could be seen that Alo might alleviate renal fibrosis by down-regulating Toll/MyD88-dependent signaling pathway.

Our research found the two pathways end inflammatory cytokines, IL-6, and TNF-α, the renal inflammatory cytokines were suggestively less intrusive in the sham and Alo groups than in the model group ($P < 0.01$), and the expression of protein for IL-6 and TNF-α was

similar in the high-dose and sham group ($P > 0.05$). This shows that astragaloside IV might prevent the release of inflammatory cytokines at the end of this pathway. By downregulating this pathway, it could hinder the release of the inflammatory cytokines and reduce inflammation, thereby reducing the expression of inflammatory cytokines in renal fibrosis.

In summary, Alo could significantly improve renal fibrosis. Its underlying mechanism may be downregulating the important node molecules in the Toll/MyD88-dependent signaling pathway and inhibiting the release of inflammatory cytokines at the end of the pathway with dose-dependent.

Financial support and sponsorship

Nil.

Conflicts of interest

There are no conflicts of interest.

REFERENCES

1. Nangaku M. Chronic hypoxia and tubulointerstitial injury: A final common pathway to end-stage renal failure. J Am Soc Nephrol 2006;17:17-25.
2. Jing H, Tang S, Lin S, Liao M, Chen H, Zhou J. The role of extracellular vesicles in renal fibrosis. Cell Death Dis 2019;10:367.
3. Shen YL, Wang SJ, Rahman K, Zhang LJ, Zhang H. Chinese herbal formulas and renal fibrosis: An overview. Curr Pharm Des 2018;24:2774-81.
4. Zhao J, Chan YC, He B, Duan TT, Yu ZL. A patent herbal drug Yi-Shen-Hua-Shi granule ameliorates C-BSA-induced chronic glomerulonephritis and inhabits TGFβ signaling in rats. J Ethnopharmacol 2019;236:258-62.
5. Wang M, Yang J, Zhou Y, et al. ShenShuai II Recipe Attenuates Apoptosis and Renal Fibrosis in Chronic Kidney Disease by Increasing Renal Blood Flow and Improving Oxygen Consumption. Evid Based Complement Alternat Med 2018; 2018:1-8.
6. Du N, Xu Z, Gao M, Liu P, Sun B, Cao X. Combination of ginsenoside Rg1 and astragaloside IV reduces oxidative stress and inhibits TGF-β1/Smads signaling cascade on renal fibrosis in rats with diabetic nephropathy. Drug Des Devel Ther 2018;12:3517-24.
7. Chen X, Yi C, Yang X, Wang X. Liquid chromatography of active principles in *Sophora flavescens* root. J Chromatogr B Analyt Technol Biomed Life Sci 2004;812:149-63.
8. Xu YQ, Jin SJ, Liu N, Li YX, Zheng J, Ma L, *et al.* Aloperine attenuated neuropathic pain induced by chronic constriction injury via anti-oxidation activity and suppression of the nuclear factor κB pathway. Biochem Biophys Res Commun 2014;451:568-73.
9. Ma NT, Zhou R, Chang RY, Hao YJ, Ma L, Jin SJ, *et al.* Protective effects of aloperine on neonatal rat primary cultured hippocampal neurons injured by oxygen-glucose deprivation and reperfusion. J Nat Med 2015;69:575-83.
10. Hu S, Zhang Y, Zhang M, Guo Y, Yang P, Zhang S, *et al.* Aloperine protects mice against ischemia-reperfusion (IR)-induced renal injury by regulating PI3K/AKT/mTOR signaling and AP-1 activity. Mol Med 2016;21:912-23.
11. Han J, Yin QH, Fang Y, Shou WQ, Zhang CC, Guo FQ. Atorvastatin protects BV2 mouse microglia and hippocampal neurons against oxygenglucose deprivationinduced neuronal inflammatory injury by suppressing the TLR4/TRAF6/NFκB pathway. Mol Med Rep 2018;18:1058-66.
12. Wang S, Schmaderer C, Kiss E, Schmidt C, Bonrouhi M, Porubsky S, *et al.* Recipient Toll-like receptors contribute to chronic graft dysfunction by both MyD88- and TRIF-dependent signaling. Dis Model Mech 2010;3:92-103.
13. Mizuguchi Y, Miyajima A, Kosaka T, Asano T, Asano T, Hayakawa M. Atorvastatin ameliorates renal tissue damage in unilateral ureteral obstruction. J Urol 2004;172:2456-9.
14. Yin W, Han J, Zhang Z, Han Z, Wang S. Aloperine protects mice against bleomycin-induced pulmonary fibrosis by attenuating fibroblast proliferation and differentiation. Sci Rep 2018;8:6265.
15. Saida K, Kamei K, Ogura M, Matsumura S, Kano Y, Sato M, *et al.* Azathioprine-induced agranulocytosis and severe alopecia after kidney transplantation associated with a NUDT15 polymorphism: A case report. Transplant Proc 2018;50:3925-7.
16. Malloy PJ, Wang J, Peng L, Nayak S, Sisk JM, Thompson CC, *et al.* A unique insertion/duplication in the VDR gene that truncates the VDR causing hereditary 1,25-dihydroxyvitamin D-resistant rickets without alopecia. Arch Biochem Biophys 2007;460:285-92.
17. Zeisberg M, Neilson EG. Mechanisms of tubulointerstitial fibrosis. J Am Soc Nephrol 2010;21:1819-34.
18. Yiu WH, Lin M, Tang SC. Toll-like receptor activation: From renal inflammation to fibrosis. Kidney Int Suppl (2011) 2014;4:20-5.
19. Lim KH, Staudt LM. Toll-like receptor signaling. Cold Spring Harb Perspect Biol. 2013; 5:1-3.
20. Wang L, Yu K, Zhang X, Yu S. Dual functional roles of the MyD88 signaling in colorectal cancer development. Biomed Pharmacother 2018;107:177-84.
21. Kawai T, Akira S. Toll-like receptors and their crosstalk with other innate receptors in infection and immunity. Immunity 2011;34:637-50.
22. Souza A C P, Takayuki T. TLR4 mutant mice are protected from renal fibrosis and chronic kidney disease progression. Physiol Rep, 2015;3:1-12.
23. Xin BM, Wang XX, Jin W, Yan HM, Cui B, Zhang XW, *et al.* Activation of Toll-like receptor 9 attenuates unilateral ureteral obstruction-induced renal fibrosis. Acta Pharmacol Sin 2010;31:1583-92.
24. Skuginna V. Toll-like receptor signaling and SIGIRR in renal fibrosis upon unilateral ureteral obstruction. PLoS One, 2011;6:3-13.
25. Ma J, Wu H, Zhao CY, Panchapakesan U, Pollock C, Chadban SJ. Requirement for TLR2 in the development of albuminuria, inflammation and fibrosis in experimental diabetic nephropathy. Int J Clin Exp Pathol 2014;7:481-95.
26. Fanton d'Andon M, Quellard N, Fernandez B, Ratet G, Lacroix-Lamandé S, Vandewalle A, *et al.* Leptospira interrogans induces fibrosis in the mouse kidney through Inos-dependent, TLR- and NLR-independent signaling pathways. PLoS Negl Trop Dis 2014;8:e2664.
27. Liu B, Ding F, Hu D, Zhou Y, Long C, Shen L, *et al.* Human umbilical cord mesenchymal stem cell conditioned medium attenuates renal fibrosis by reducing inflammation and epithelial-to-mesenchymal transition via the TLR4/NF-κB signaling pathway *in vivo* and *in vitro*. Stem Cell Res Ther 2018;9:7.
28. Wermuth PJ, Jimenez SA. Gadolinium compounds signaling through TLR4 and TLR7 in normal human macrophages: Establishment of a proinflammatory phenotype and implications for the pathogenesis of nephrogenic systemic fibrosis. J Immunol 2012;189:318-27.